

© 2022 IEEE. Personal use of this material is permitted. Permission from IEEE must be obtained for all other uses, in any current or future media, including reprinting/republishing this material for advertising or promotional purposes, creating new collective works, for resale or redistribution to servers or lists, or reuse of any copyrighted component of this work in other works.

Inline Waveguide Filter With Transmission Zeros Using a Modified-T-Shaped-Post Coupling Inverter

Muhammad Yameen Sandhu ¹, Senior Member, IEEE, Maciej Jasinski ², Graduate Student Member, IEEE, Adam Lamecki ³, Senior Member, IEEE, Roberto Gómez-García ⁴, Senior Member, IEEE, and Michal Mrozowski ⁵, Fellow, IEEE

Abstract—This letter reports the design techniques for a class of inline waveguide bandpass filters with sharp-rejection capabilities at the lower stopband based on a novel nonlinear-frequency-variant-coupling (NFVC) structure. The proposed NFVC consists of a modified-T-shaped metallic post (MTP) that is placed at the center of the waveguide broad wall with its open arms lying along the waveguide width. The engineered NFVC structure produces a first-order bandpass filtering transfer function with a pair of transmission zeros (TZs) located below the passband range. To demonstrate the usefulness of the proposed NFVC inverter, a 9.9-GHz third-order inline waveguide bandpass filter prototype with two TZs is developed and tested. It consists of two half-wavelength cavity resonators coupled together via the conceived MTP coupling structure. The measured results are in close agreement with the electromagnetic (EM) simulated ones, thus validating the devised waveguide filter design principle.

Index Terms—3-D filter, bandpass filter, coupling-matrix synthesis, frequency-dependent coupling, inline filter, microwave filter, transmission zero (TZ), waveguide filter.

I. INTRODUCTION

TRANSCEIVER radio frequency (RF) front-end chains in modern wireless communication systems require highly selective RF bandpass filters to properly acquire the desired frequency signals while efficiently rejecting adjacent channel interference/jamming and noise. Transmission zeros (TZs) are commonly exploited to increase the selectivity in bandpass filters, and they can be realized by cross couplings between nonadjacent resonators [1], [2], [3], by overmoded

Manuscript received 2 June 2022; revised 16 July 2022 and 22 August 2022; accepted 9 September 2022. This work was supported in part by the Polish National Science Centre under Grant UMO-2019/33/B/ST7/00889, in part by the Polish National Agency for Academic Exchange (NAWA) under Agreement PPN/ULM/2019/1/00079/U/00001, and in part by the Gdańsk University of Technology through the Excellence Initiative—Research University (ARGENTUM) under Grant DEC-54/2020/IDUB/I.3.3. (Corresponding author: Muhammad Yameen Sandhu.)

Muhammad Yameen Sandhu is with the Faculty of Electronics, Telecommunications, and Informatics, Gdańsk University of Technology, 80-233 Gdansk, Poland, and also with the Department of Electrical Engineering, Sukkur IBA University, Sukkur 65200, Pakistan (e-mail: muhammad.sandhu@pg.edu.pl).

Maciej Jasinski is with the Department of Microwave and Antenna Engineering, Gdańsk University of Technology, 80-233 Gdansk, Poland.

Adam Lamecki and Michal Mrozowski are with the Faculty of Electronics, Telecommunications, and Informatics, Gdańsk University of Technology, 80-233 Gdansk, Poland (e-mail: adam.lamecki@iee.org; m.mrozowski@iee.org).

Roberto Gómez-García is with the Department of Signal Theory and Communications, Polytechnic School, University of Alcalá, 28871 Alcalá de Henares, Spain (e-mail: roberto.gomez.garcia@iee.org).

Color versions of one or more figures in this letter are available at <https://doi.org/10.1109/LMWC.2022.3208141>.

Digital Object Identifier 10.1109/LMWC.2022.3208141

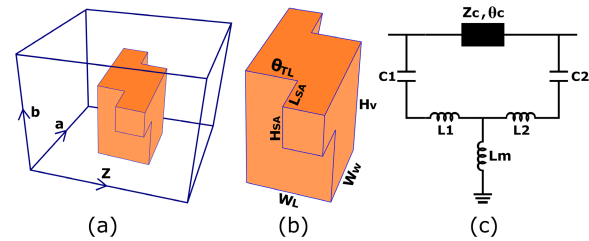


Fig. 1. Proposed MTP NFVC inverter. (a) MTP placed inside a waveguide. (b) MTP with an indication of geometrical variables. (c) Equivalent circuit of the MTP NFVC inverter.

resonant cavities [4], [5], [6], or by frequency-variant couplings (FVCs). In waveguides, an FVC could be implemented by means of different structures, such as a single partial-height metallic post [7], [8], [9], [10], a pair of closely spaced posts [11], [12], a series or shunt stub [13], [14], or with more complex resonant diaphragms [15], [16], [17], [18], [19], [20]. Various synthesis procedures to design filters with FVCs have been reported in the technical literature [21], [22], [23]. In [24], a detailed synthesis method based on a coupling-matrix formulation is presented to design bandpass filters with arbitrary frequency-variant reactive-type coupling structures. The design of an inline generalized Chebyshev waveguide bandpass filter with dual-post novel nonlinear-frequency-variant-couplings (NFVCs) by using the referred coupling-matrix-based synthesis approach is demonstrated in [25].

As a further contribution, the design of a class of inline generalized Chebyshev waveguide bandpass filters based on an alternative NFVC structure is reported in this letter. The proposed NFVC inverter consists of a modified-T-shaped metallic post (MTP) that is placed inside the waveguide, where the open arms of the post are lying along the width of the waveguide. This type of NFVC inverter is capable of producing two TZs along with a pole that is located above the pair of TZs. Note that although the referred case where the pole is located above the TZs is considered here, the pole could also be positioned either below or in between the TZs. Using this NFVC inverter to couple two half-wavelength cavity resonators, a third-order waveguide bandpass filter prototype with two TZs is designed, fabricated, and tested to verify the practical usefulness of the proposed NFVC structure.

II. MODIFIED T-SHAPED NFVC INVERTER

An MTP placed inside a waveguide, as shown in Fig. 1(a) and (b), behaves as an NFVC inverter that can produce two TZs along with a transmission pole in its frequency

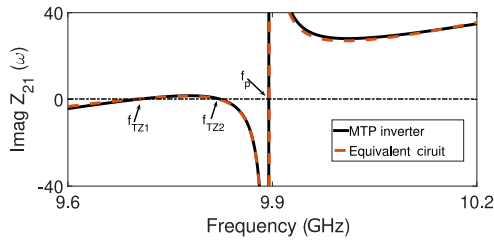


Fig. 2. Comparison of the transimpedance (Z_{21}) parameter of the MTP NFVC inverter using its physical structure in Fig. 1(b) ($W_w = 3.4$ mm, $W_L = 4.3$ mm, $H_v = 5.24$ mm, $L_{SA} = 4.38$ mm, $\theta_{TL} = 2.3$ mm, $H_{SA} = 2.44$ mm, and two tuning screws with radius and depth of 1.5 mm being placed at the edges of the sidearms inside a WR90 waveguide) and its equivalent circuit in Fig. 1(c) ($L_1 = L_2 = 5.71$ nH, $C_1 = C_2 = 44$ nF, $Z_c = 50$ Ω , and $\theta_c = 23.8$ at 9.9 GHz).

response. The plot shown in Fig. 2, which corresponds to the transimpedance parameter (Z_{21}) for an example of the devised MTP NFVC inverter and its equivalent circuit, confirms the creation of a TZ pair and a pole located at a frequency above the two TZs. This structure can be modeled as two mutually coupled series-type resonators separated by a section of transmission line (TL), as can be seen in the equivalent circuit depicted in Fig. 1(c). Here, the short-ended vertical post is modeled as a mutual inductive-type coupling (L_M), the open-ended horizontal arms are represented as the inductances (L_1 and L_2) of the series resonators, the gaps between the open ends and the walls of the waveguide cavity are approximated as the capacitances (C_1 and C_2) of the series resonators, and the longitudinal separation of the open arms is modeled as a TL section between the resonators. For the given structure, the pole is located above the pair of TZs. In fact, a simple T-shaped inverter, that is, $\theta_{TL} = 0$, also produces two TZs and a pole, but in such cases, the pole is always located between the pair of TZs. A TL section—longitudinal separation of the open-ended horizontal arms of the post—is then necessary to shift the pole location above the pair of TZs. Alternatively, the simple T-bar can be rotated 90° so that the open ends of the horizontal bar point along the direction of the signal propagation in the waveguide. In practice, this would result in an increase in the physical size of the inverter. Furthermore, as an added effect for such a case, the open ends of the horizontal bar would penetrate deep inside the adjacent cavities, thus significantly detuning the adjacent cavities. The equivalent circuit derived for the MTP inverter suggests that for the provided circuit arrangement, the pole could only be located above the TZ pair if there is a small TL section between the mutually coupled series-type resonators. Similarly, the locations of the TZs can be controlled by simultaneously adjusting the element values of the series resonators and their mutual coupling. To confirm this and to visualize the effect of the different physical dimensions of the MTP on the location of the pole and the TZs, a parametric sweep of the height of the vertical post (H_v), the width of the vertical post along the waveguide width (W_w), the length of the side arms (L_{SA}), and the additional TL section between the side arms (θ_{TL}) has been carried out using the electromagnetic (EM) simulator Ansys high frequency structure simulator (HFSS). In all cases, the MTP was placed in a standard WR-90 waveguide having a width of 22.86 mm and a height of 10.16 mm. The short-ended rectangular vertical post is 4-mm long, 3-mm wide along the width of the waveguide, and 3.2-mm wide along the length of the waveguide. The side arms are 4.7-mm long and 2-mm

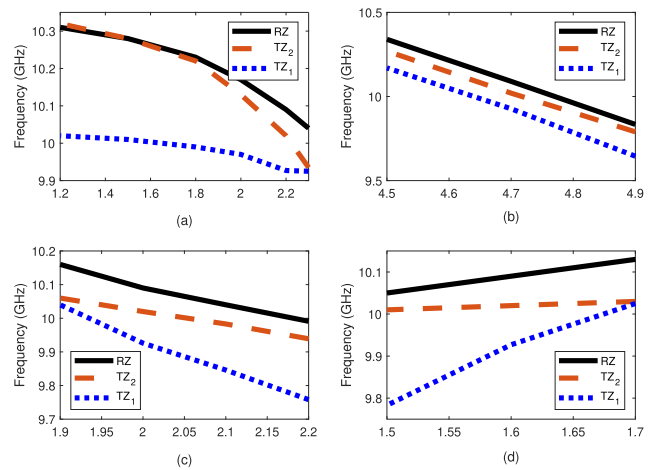


Fig. 3. Influence of the different MTP dimensions on the spectral locations of the TZs (TZ_1 and TZ_2) and the pole (RZ). MTP is placed inside a WR90 waveguide with width $a = 22.86$ mm and height $b = 10.16$ mm. (a) Longitudinal distance (θ_{TL}) between side arms-mm. (b) Length of side arms of the post (L_{SA})-mm. (c) Height of the vertical post (H_v)-mm. (d) Width (W_w) of the vertical post-mm.

thick, and they are vertically aligned with the top surface of the main post. The center-to-center separation between the side arms of the post along the length of the waveguide is 2.2 mm. It is evident from the results shown in Fig. 3(a) that by introducing a small TL section (θ_{TL}) between the side arms, the pole frequency is reallocated above the TZs. Besides, by further increasing its length, the pole frequency moves further away from the TZ pair. The length of side arms could be mainly used to allocate the TZs and the pole in a widely adjustable spectral range as revealed by Fig. 3(b). Furthermore, the width and the height of the short-ended vertical post serving as mutual coupling are useful parameters to control the frequency separation between the two TZs. Note that the two TZs could be brought closer to each other by either decreasing the height of the vertical post or by increasing the width of the vertical post along the waveguide width as demonstrated in Fig. 3(c) and (d), respectively. Note that the TZ pair could be relocated to above the pole location by simultaneously increasing the width (W_w) of the vertical post and decreasing the length of side arms (L_{SA}). It must be remarked upon that a comparable response could be obtained by replacing the MTP with a pair of closely spaced partial-height posts, as reported by Sandhu *et al.* [12]. However, considering practical reasons, the current approach may be more suitable since very closely spaced posts are difficult to fabricate. Besides, it is tedious to place tuning screws in a tight space to allow postfabrication tuning for such an arrangement. A performance comparison of the proposed MTP inverter with related prior-art inverter configurations—in terms of the number of TZs and created additional poles, the minimum number of resonators required to implement the coupling inverter, need of cross couplings, and flexibility of locating the TZ either below or above the passband—is presented in Table I.

III. FILTER DESIGN EXAMPLE

To validate the concept, a third-order bandpass filter with 150-MHz bandwidth, 9.9-GHz center frequency, and two TZs located in the lower stopband at 9.675 and 9.78 GHz has been designed. This filter prototype consists of two WR90 half-wavelength cavity resonators that are coupled through the conceived MTP NFVC network. To design the filter as

TABLE I
COMPARISON WITH RELATED PRIOR-ART INVERTERS

Parameter	[7]	[11]	[3]	This work
Number of TZs	1	1	1	2
Additional Pole	No	Yes	No	Yes
Resonators for third-order filter	2	2	3	2
TZ placement	Either side	Either side	Either side	Both sides
Cross coupling needed	No	Yes	Yes	No

per the given specifications and topology, a coupling matrix is synthesized using the approach in [24]. The synthesis is carried out directly in the passband domain and by using the coupling-network model shown in Fig. 1(c). The synthesis process involves solving a structured inverse nonlinear eigenvalue problem. Based upon the coupling-matrix entries and prespecified TZ locations, the MTP NFVC inverter is extracted to realize a pole and two TZs. Specifically, such process provides the electrical length of waveguide cavities $\theta_{\text{res}} = 177.3^\circ$, the TL section length $\theta_c = 2.62^\circ$ with $Z_c = 47.44 \Omega$, the external coupling $K_{\text{in,out}} = 10.47$, $L_1 = 0.42$ nH, $L_2 = 0.355$ nH, $C_1 = 0.598$ pF, $C_2 = 0.7023$ pF, and $L_m = 0.034$ nH. To design the MTP NFVC inverter, a parametric sweep of the 3-D structure of the post is carried out by using the commercial 3-D EM simulator HFSS. Initially, a simple T-shaped post is designed to realize a pole surrounded by a pair of TZs. The length of the open-ended arms of the post is exploited to control the locations of the TZs, whereas the height and thickness of the vertical post could be utilized to modify the frequency spacing between the TZs. Once the TZ locations are tuned, then the open-ended arms of the post are moved apart along the signal propagation direction to introduce the TL section between the open ends of the post. Adding such a TL section allows us to flip the pole frequency above the TZ pair. Once the MTP NFVC inverter is extracted, then the remaining waveguide cavity resonators and external coupling inverters are derived using standard waveguide filter design theory. The external couplings are realized as H-plane inductive window couplings. Fine numerical tuning is finally performed using the zero-pole optimization technique of the commercial finite element method (FEM)-based microwave electronic design automation (EDA) software InvenSim. The *E*-field pattern of the final optimized filter is shown in Fig. 4.

IV. EXPERIMENTAL VALIDATION

The photograph of the final fabricated prototype is given in Fig. 5. The filter is manufactured in two pieces—body and top lid—using computer numerical control (CNC) machining. The post is fabricated separately and then fit in the base wall of the filter and heat-treated to solidify the connection to the base unit. The post dimensions are as follows: $W_w = 3.76$ mm, $W_L = 4.2$ mm, $H_v = 5.24$ mm, $L_{\text{SA}} = 4.45$ mm, $\theta_{\text{TL}} = 2.2$ mm, and $H_{\text{SA}} = 2.44$ mm. Tuning screws with a diameter of 3 mm are placed at the center of waveguide cavities, at the external coupling windows, and at the edges of the side arms of the MTP to allow postfabrication tuning so that to compensate for manufacturing inaccuracies. A comparison between the EM-simulated and measured power transmission and reflection responses of the built third-order bandpass filter prototype is shown in Fig. 6. The measured prototype has a minimum in-band return and insertion loss of 19 and 0.56 dB, respectively, 135-MHz bandwidth, and a center frequency of

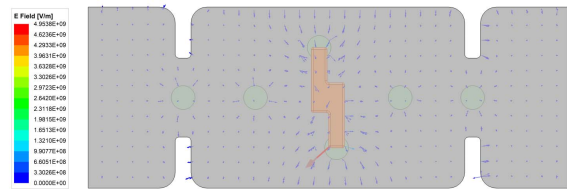


Fig. 4. *E*-field pattern for the simulated third-order filter prototype.

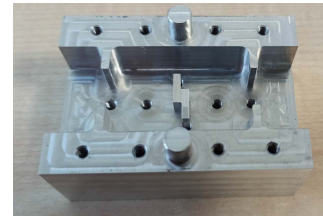


Fig. 5. Photograph of the manufactured prototype (internal dimensions: $22.86 \times 36.58 \times 10.16$ mm³).

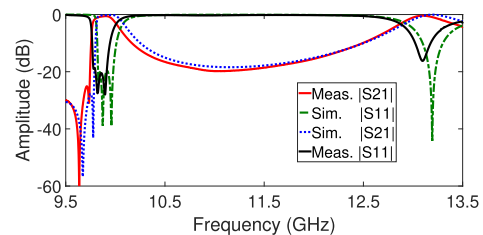


Fig. 6. EM-simulated and measured power transmission ($|S_{21}|$) and reflection ($|S_{11}|$) responses of the manufactured prototype.

9.847 GHz. The spurious resonance at about 13 GHz is caused by the MTP inverter. As can be seen, a reasonable agreement is obtained between EM-simulated and experimental results in terms of passband return-loss level, filter bandwidth, presence of two TZs below the passband, and spurious performance, so that the engineered waveguide filter principle is fairly verified. It is observed that the whole filter response is slightly shifted to a lower frequency due to manufacturing errors in the dimensions of the MTP inverter and the outer cavities. Some minor discrepancy in terms of passband insertion loss is attributed to the added lossy tuning screws. Note also that the filter pole associated with the MTP has a lower quality factor Q (2963) when compared to a regular cavity resonator. This results in a reduced average unloaded Q for the filter of 5100. Nevertheless, the measured prototype verifies this design principle of the waveguide filter.

V. CONCLUSION

This letter presents a design technique to implement inline waveguide bandpass filters with two TZs at the lower passband side based on a new class of MTP NFVC inverter. The proposed inverter produces a transmission pole located above a pair of TZs, unlike its simple T-shaped postinverter counterpart where the pole is located between the two TZs. This is achieved by moving apart the arms of the T-shaped inverter, which allows reallocating the pole above the TZ pair. A 9.9-GHz proof-of-concept prototype of a third-order waveguide bandpass filter based on the proposed MTP NFVC inverter is designed, fabricated, and measured to validate the engineered filter principle and design theory.

REFERENCES

- [1] M. Latif, G. Macchiarella, and F. Mukhtar, "A novel coupling structure for inline realization of cross-coupled rectangular waveguide filters," *IEEE Access*, vol. 8, pp. 107527–107538, 2020.
- [2] U. Jankovic, N. Mohottige, and D. Budimir, "Design of ultra compact pseudo-elliptic inline waveguide bandpass filters using inductive bypass coupling for various specifications," in *Proc. Act. Passive RF Devices*, 2017, pp. 1–6.
- [3] M. Y. Sandhu and I. C. Hunter, "Miniaturized dielectric waveguide filters," *Int. J. Electron.*, vol. 103, no. 10, pp. 1776–1787, Oct. 2016.
- [4] M. A. Chaudhary and M. M. Ahmed, "Inline waveguide pseudo-elliptic filters using non-resonating modes with folded-waveguide resonators," *IEEE Access*, vol. 9, pp. 140841–140852, 2021.
- [5] R. V. Snyder, G. Macchiarella, S. Bastioli, and C. Tomassoni, "Emerging trends in techniques and technology as applied to filter design," *IEEE J. Microw.*, vol. 1, no. 1, pp. 317–344, Jan. 2021.
- [6] S. Bastioli and R. V. Snyder, "Nonresonating modes do it better!: Exploiting additional modes in conjunction with operating modes to design better quality filters," *IEEE Microw. Mag.*, vol. 22, no. 1, pp. 20–45, Jan. 2021.
- [7] C. Tomassoni and G. Macchiarella, "A new resonant coupling structure for inline waveguide filters with transmission zeros," in *IEEE MTT-S Int. Microw. Symp. Dig.*, Nov. 2021, pp. 297–299.
- [8] U. Rosenberg and S. Amari, "A novel band-reject element for pseudo-elliptic bandstop filters," *IEEE Trans. Microw. Theory Techn.*, vol. 55, no. 4, pp. 742–746, Apr. 2007.
- [9] P. Zhao and K. Wu, "Waveguide filters with central-post resonators," *IEEE Microw. Wireless Compon. Lett.*, vol. 30, no. 7, pp. 657–660, Jul. 2020.
- [10] M. Y. Sandhu, Z. Ahmed, S. Hyder, and S. Afridi, "Inline integrated ceramic waveguide bandpass filter with N+1 finite transmission zeros," *IETE J. Res.*, vol. 2020, pp. 1–7, Aug. 2020, doi: 10.1080/03772063.2020.1808094.
- [11] C. Tomassoni and R. Sorrentino, "A new class of pseudoelliptic waveguide filters using dual-post resonators," *IEEE Trans. Microw. Theory Techn.*, vol. 61, no. 6, pp. 2332–2339, Jun. 2013.
- [12] M. Sandhu, A. Lamecki, R. Gómez-García, and M. Mrozowski, "Quasi-elliptic-type inline waveguide filters with mutually-coupled rotated-dual-post frequency-variant coupling inverters," in *Proc. IEEE MTT-S Int. Conf. Numer. Electromagn. Multiphys. Modeling Optim.*, Jul. 2022.
- [13] L. Szydlowski and M. Mrozowski, "A self-equalized waveguide filter with frequency-dependent (resonant) couplings," *IEEE Microw. Wireless Compon. Lett.*, vol. 24, no. 11, pp. 769–771, Nov. 2014.
- [14] S. Amari and J. Bornemann, "Using frequency-dependent coupling to generate finite attenuation poles in direct-coupled resonator bandpass filters," *IEEE Microw. Guided Wave Lett.*, vol. 9, no. 10, pp. 404–406, Oct. 1999.
- [15] V. Zemlyakov, S. Krutiev, M. Tyaglov, and V. Shevchenko, "A design of waveguide elliptic filter based on resonant diaphragms with a complex aperture," *Int. J. Circuit Theory Appl.*, vol. 47, no. 1, pp. 55–64, Jan. 2019.
- [16] P. Kozakowski, A. Lamecki, M. Mongiardo, M. Mrozowski, and C. Tomassoni, "Computer-aided design of in-line resonator filters with multiple elliptical apertures," in *IEEE MTT-S Int. Microw. Symp. Dig.*, Jun. 2004, vol. 2, no. 2, pp. 611–614.
- [17] Y. Zhang, H. Meng, and K.-L. Wu, "Direct synthesis and design of dispersive waveguide bandpass filters," *IEEE Trans. Microw. Theory Techn.*, vol. 68, no. 5, pp. 1678–1687, May 2020.
- [18] U. Rosenberg, S. Amari, and F. Seyfert, "Pseudo-elliptic direct-coupled resonator filters based on transmission-zero-generating irises," in *Proc. 40th Eur. Microw. Conf.*, Sep. 2010, pp. 962–965.
- [19] C. A. Leal-Sevillano, J. R. Montejo-Garai, J. A. Ruiz-Cruz, and J. M. Rebollar, "Wideband equivalent circuit for multi-aperture multi-resonant waveguide irises," *IEEE Trans. Microw. Theory Techn.*, vol. 64, no. 3, pp. 724–732, Mar. 2016.
- [20] A. Bage, S. Das, L. Murmu, U. Pattapu, and S. Biswal, "Waveguide bandpass filter with easily adjustable transmission zeros and 3-dB bandwidth," *Int. J. Electron.*, vol. 105, no. 7, pp. 1170–1184, Jul. 2018.
- [21] L. Szydlowski, A. Lamecki, and M. Mrozowski, "A novel coupling matrix synthesis technique for generalized Chebyshev filters with resonant source-load connection," *IEEE Trans. Microw. Theory Techn.*, vol. 61, no. 10, pp. 3568–3577, Oct. 2013.
- [22] Y. Zhang and K.-L. Wu, "General method for synthesizing dispersive coupling matrix of microwave bandpass filters," *Int. J. Microw. Wireless Technol.*, vol. 14, no. 3, pp. 379–386, 2021.
- [23] G. Macchiarella, G. G. Gentili, N. Delmonte, L. Silvestri, and M. Bozzi, "Design of inline waveguide filters with frequency-variant couplings producing transmission zeros," *IEEE Trans. Microw. Theory Techn.*, vol. 69, no. 8, pp. 3746–3758, Aug. 2021.
- [24] M. Mul, A. Lamecki, R. Gomez-Garcia, and M. Mrozowski, "Inverse nonlinear eigenvalue problem framework for the synthesis of coupled-resonator filters with nonresonant nodes and arbitrary frequency-variant reactive couplings," *IEEE Trans. Microw. Theory Techn.*, vol. 69, no. 12, pp. 5203–5216, Dec. 2021.
- [25] M. Sandhu, M. Mrozowski, A. Lamecki, and R. Gómez-García, "Compact quasi-elliptic-type inline waveguide bandpass filters with nonlinear frequency-variant coupling inverters," *TechRxiv*, 2022.